Oleg DEKUSHA[1], Sergiy KOBZAR[2] , Serhii IVANOV[3]

Science supervisor: Svitlana KOVTUN[4]

CALORIMETRIC METHOD FOR MEASURING THE EMISSIVITY OF COATINGS AND MATERIAL SURFACES

Summary: The aim of the work is to demonstrate the possibility of using the calorimetric method for measuring the emission factor without vacuuming the volume of the measuring chamber, taking into account the heat exchange from the radiator to the surface of the sample through the air layer, is substantiated.

Keywords: emissivity measurement, calorimetric measurement methods, emissivity coefficient

KALORYMETRYCZNA METODA DO MIERZENIA EMISYJNOŚCI POKRYĆ ORAZ POWIERZCHNI MATERIAŁU

Streszczenie: Celem pracy było pokazanie możliwości użycia metod kalorymetrycznych do pomiaru emisji czynnika bez pomiarów z zastosowaniem komory próżniowej. W zaproponowanej metodzie uwzględnia się wymianę ciepła z radiatora na powierzchnie próbki przez warstwę powietrza; to podstawowa idea proponowanego podejścia.

Słowa kluczowe: pomiary emisyjności, metoda pomiarów kalorymetrycznych, współczynnik emisyjności

1. Introduction

For real bodies, the emissivity is a complex function that depends on the nature of the radiating body, its temperature, the surface condition, and for metals - on the degree of oxidation of this surface.

[1] Institute of Engineering Thermophysics of NAS of Ukraine, Monitoring and optimization of thermal processes dep, ODekusha@nas.gov.ua
[2] Institute of Engineering Thermophysics of NAS of Ukraine, High-Temperature Thermogasdynamics dep, SKobzar@nas.gov.ua
[3] Institute of Engineering Thermophysics of NAS of Ukraine, Monitoring and optimization of thermal processes dep, IvanovSO@nas.gov.ua
[4] Doctor of Science, Institute of Engineering Thermophysics of NAS of Ukraine, Monitoring and optimization of thermal processes dep, KovtunSI@nas.gov.ua

Determination of the emissivity is relevant for a lot of research cases, in particular when determining the properties of energy efficient windows, coatings and composite materials in space technology, in pyrometric measurements and thermal imaging [1 ... 6].

Among of the emissivity measurement experimental methods are worth to point the following: radiation method, calorimetric method, a method of regular mode, continuous heating method with constant speed.

The radiation method is a relative method [7]. It based on the comparison of the radiation of the body under study with the radiation of an absolutely black or other reference body with a known radiation coefficient.

The calorimetric method based on the direct measurement of the radiation flux from the examined sample [7]. This method is absolute. The emissivity of sample is determined by the Stefan-Boltzmann law.

In all methods, the heat exchange by convection and the heat conductivity of the air should be very small compared with radiation.

Stationary laboratory devices, as a rule, provide measurements in a wide temperature range with vacuuming a working chamber [8] for reduce the conductive-convective component of heat exchange. In this device, the radiating surface with known characteristics and the receiving surface of the test sample are parallel and placed at relatively small distance (several millimeters) in the vacuumed space.

The aim of the work is to demonstrate the possibility of using the calorimetric method for measuring the emission factor without vacuuming the volume of the measuring chamber, taking into account the heat exchange

2. Method description and Simulation model

Device without vacuuming the working chamber, which includes the emitter and the reference and tested samples placed on the heat flux sensors installed on the cooled heat exchanger. The working chamber of such device is formed by a top emitter, a bottom heat exchanger and polished side walls which have a heat-exchanger temperature. In such device, the emitter is placed at a sufficiently large distance from the sensors with samples, so the influence of conductive heat exchange is greatly reduced.

The simplified equation for heat flux measuring with the radiation method of supplying thermal energy is written based on the Stefan-Boltzmann law [5] under the assumption that conductive-convective heat exchange through the air is absent and boundary effects and distortions of the thermal field are not taken into account through them:

$$q = \varepsilon_{com} \cdot \varphi \cdot \sigma \cdot (T_1^4 - T_3^4) \tag{1}$$

Where φ – angle coefficient of radiation, which takes into account the shape and size of the surfaces involved in the heat exchange, their mutual arrangement; σ – Stefan-Boltzmann constant; T_1 – a temperature of the upper end surface; T_3 – a temperature

of the bottom end surface; ε_{com} – complex emissivity which can be found by equation (2):

$$\varepsilon_{com} = \left(\frac{1}{\varepsilon_3} + \frac{F_3}{F_1} \left(\frac{1}{\varepsilon_1} - 1 \right) \right)^{-1} \tag{2}$$

Formation of the heat flux occurs by maintaining the difference in temperature of the source of thermal energy and heat transfer, taking into account the energy emitted by the surfaces of heat exchange, their mutual arrangement and thermal radiation characteristics.

The accuracy of measurements in devices of this type depends on the influence of conductive-convective heat transfer, and on the homogeneity of the measured density of the heat flux. To minimize the methodical component of the measurement error, it is necessary that the samples and sensors be in the zone of one-dimensional heat flux, so that the measured density of the heat flux will be equal to the density of the heat flux through the sample.

Simulation of radiation-convective heat exchange in the device was done to determine the zone with the permissible unevenness of the heat flux and to estimate the influence of conductive-convective heat transfer on the accuracy of measurement.

The simulations were carried out using the ANSYS CFX software package. The object of the simulation is a closed cylindrical cavity, which simulates the device [9]. The cavity is filled with atmospheric air.

The radius of the cylinder is r = 95 mm, the height H = 260 mm. The top surface was heated, and the bottom perceived heat (radiation, conductive and convective). Material of the side surface - polished aluminum.

An unstructured combined grid, built using the ANSYS CFX Mesh and object of the simulation are presented on Fig. 1.

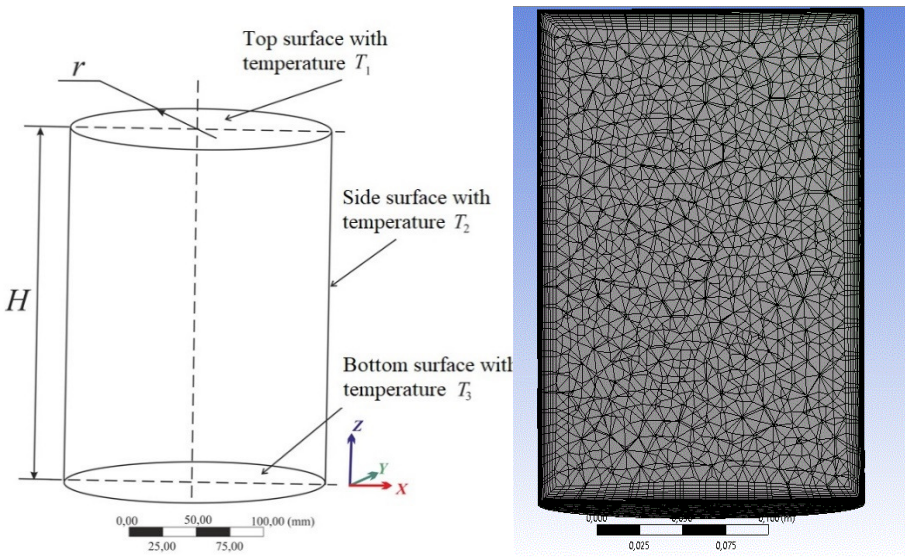

Figure 1. Object of the simulation and Grid mesh

Simulation mesh parameters shown in Table 1.

Table 1. Simulation mesh parameters

Inflation	Method	Smooth transition
	Transition Ratio	0.2
	Maximum Layers	15
	Growth Rate	1,2
Max Face Size, m		1,0 E-2
Max Size, m		1,0 E-2
Number of Nodes		47 **thousands**
Number of Elements		125 **thousands**

The boundary conditions of the simulation are given in Table 2.

Table 2. Boundary conditions

Border	Temperature, K	Emissivity
Top Surface	393 … 1000	0,95
Side Surface	300	0,1 … 0,2
Bottom Surface	300	0,95

The air was considered an ideal gas. The dependence of isobaric heat capacity on temperature was determined by a polynomial dependence:

$$\frac{C_p}{R} = a_o + a_1 \cdot T + a_2 \cdot T^2 + a_3 \cdot T^3 + a_4 \cdot T^4 , \quad (3)$$

where R – gas constant; $a_0 \ldots a_4$ – polynomial coefficients.

The dependence of the coefficient of dynamic viscosity and the thermal conductivity of air on the temperature was given by Sutherland's formulas:

$$\mu = \mu_0 \left(\frac{T}{T_0} \right)^n \frac{T_o + C_S}{T + C_S} \quad (4)$$

$$\lambda = \lambda_0 \left(\frac{T}{T_0} \right)^n \frac{T_o + C_{S1}}{T + C_{S1}} \quad (5)$$

where μ_0, λ_0 – base values of the coefficients of dynamic viscosity and thermal conductivity; $T_0 = 273{,}15$ K – base temperature of the air.

The Navier-Stokes equations averaged by Reynolds were solved for viscous heat conducting gas in stationary formulation using a complete energy conservation equation as a heat exchange model

The effect of gravity was taken into account in the direction of the Z axis.

Radiation heat exchange was modeled using the Discrete Transfer model.

The required diffusion reflection coefficient R_d for the side surface (aluminum) is taken to be equal to 0.1, according to the results showed in [10].

3. Simulation results and verification of the model

The vector field (Fig. 2) and the field of values of air velocity (Fig. 3) shows in the central section of the cylinder. As can be seen from Fig.2, a vortex structure is formed in the lower angular zone. Near the side surface there is a downstream, and in the central zone - lifting.

Near the bottom surface, the field of velocity along the longitudinal axis is fairly uniform, with the value w being about 1.5 mm/s. It should be noted that the impact of convection on the total heat flux is rather insignificant. The total contribution to the total heat exchange of convection and the thermal conductivity does not exceed 0.1%, that is, it can be assumed that the entire heat flux is transferred by radiation.

The temperature field of the air medium at the central intersection of the cylindrical cavity at a temperature of the upper end surface T_1 = 175 ° C. As can be seen from the Fig. 4, the main longitudinal temperature gradient is located near the Top end surface and at a distance from it, the air temperature changes slightly.

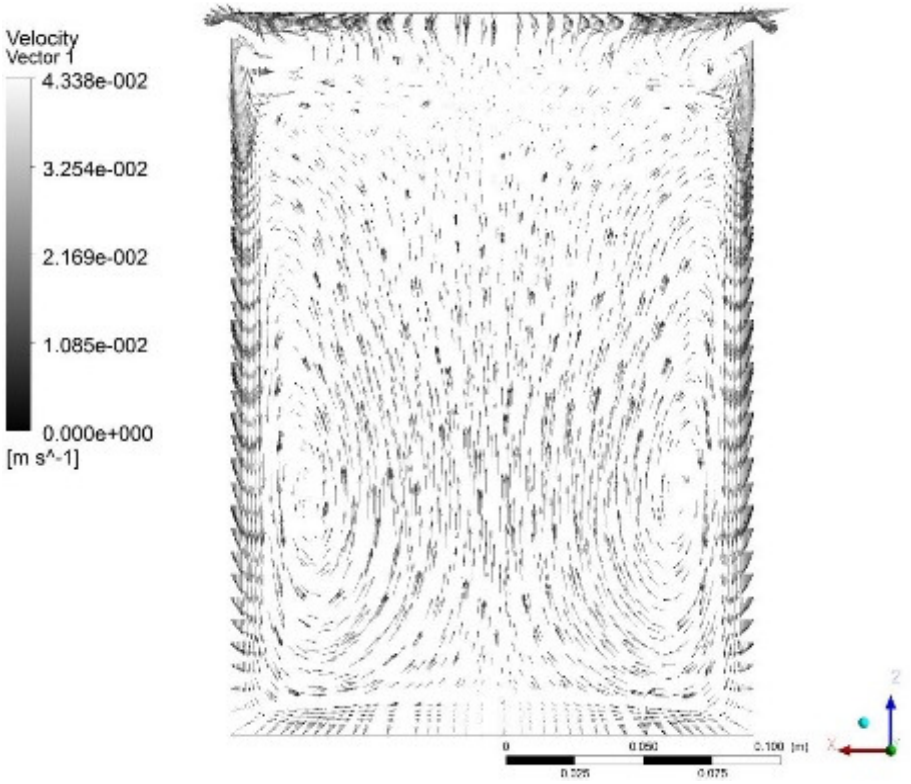

Figure 2. Air velocity in the central section of the cylinder

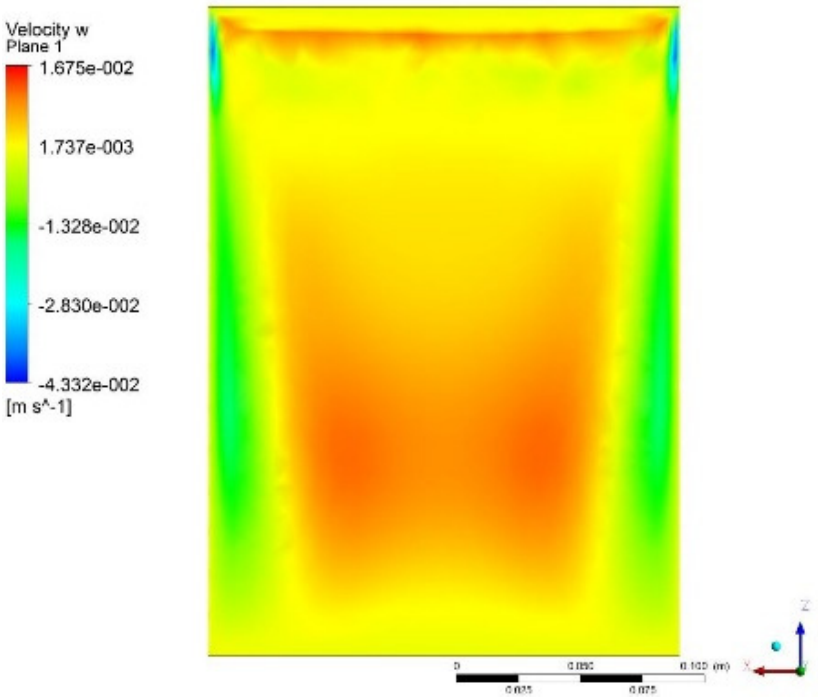

Figure 3. The value of the axial velocity in the central section of the cylinder

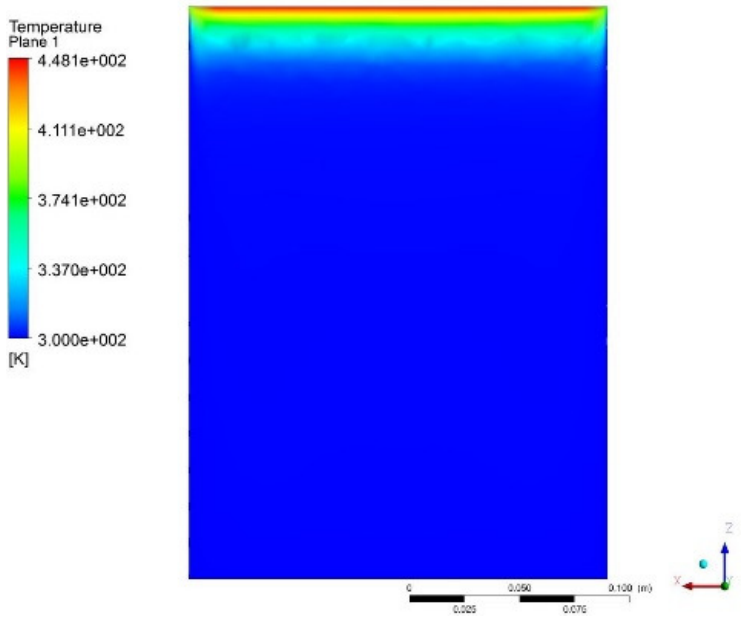

Figure 4. Temperature field in the cylinder cavity (central section)

Number of rays in the proposed simulation model $n = 32$ was used [11].

For verification of the simulation, the results of experiments were taken [9], a comparison of the results of the experiment and the simulation at a temperature of the upper face surface 175 °C and a variation in the calculations of the side surface emissivity was made: its values were set to 0,1 and 0,2. The results are shown on Fig.5.

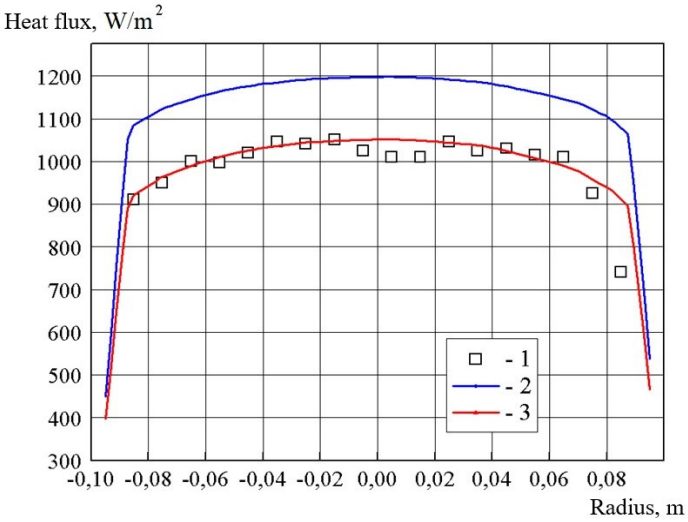

Figure 5. Radial distribution of the heat flux on the bottom surface of the cylinder at a temperature of the Top surface T_1 = 175 ° C and diffuse reflection coefficient R_d = 0,1: 1 - experiment; 2, 3 - calculation at the value of side surface emissivity ε_2, respectively, 0.1 and 0.2.

First, it should be noted that the distribution pattern is practically the same for experiments and calculations. As can be seen from the Fig. 5, the quantitative coincidence of the calculated and experimental results takes place when the level of emissivity of the side surface ε_2 = 0,2.

It can be assumed that in the central zone of the bottom heat exchanger with a radius of 0.06 m, which is 63% of the radius of the side polished cylinder, the uneven distribution of the heat flux does not exceed ± 2%, and this area is suitable for measurement.

In real conditions, sensor only partially covers the lower end surface of the cylinder (Fig. 6, green). At the same time, emissivity of the surfaces differ significantly: for the sensor surface ε = 0.95 and the rest of the surface ε = 0.2. Despite the low temperature of the lower end surface (300 K), this difference, however, can affect the total beam heat transfer in the cylinder cavity due to the redistribution of heat fluxes. To calculate this case, a computer model was modified - with a selection of 0.19x0.03m on the lower surface of the calculation area.

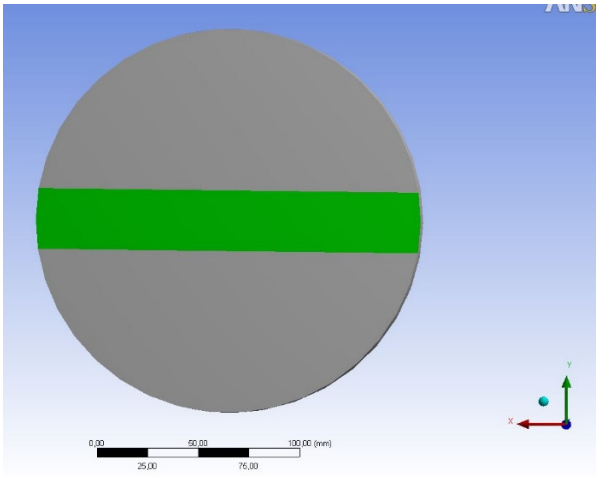

Figure 6. Variant where the sensor only partially covers the lower end surface

The results of simulations and their comparison with the results of experiments and preliminary calculations (for the case where the sensor model occupies the entire lower surface) for different heater temperatures are shown in Fig. 7

As can be seen from the Fig. 7, taking into account the difference in the degree of blackness of the sensor and the rest of the lower surface of the cylinder leads to an increase in heat flow, but this increase is negligible, and amounts to 3.8… 3.9%.

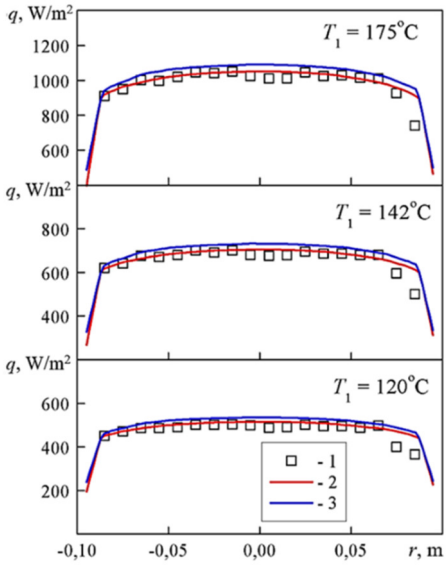

Figure 7. Radial distribution of the specific heat flux on the lower end surface of the cylinder different values of the temperature of the upper end surface T1.
1 - experiment; 2 - calculation at the emissivity of the entire lower surface $\varepsilon^3 = 0,95$; 3 - calculation for the emissivity of the sensor surface $\varepsilon = 0,95$ and the rest of the surface $\varepsilon = 0,2$

4. Calorimetric device for measuring the emissivity of coatings and material surfaces

Taking into account the results obtained during simulation, modernized the measurement system RGU-2 Fig. 8 for calibrating the heat flux sensors and measuring the emissivity of coatings and material surfaces. Technical Specifications presented Table 3.

After modernization increased range of measured emissivity coefficient up to 0.040…0.99.

Table 4. Technical Specifications

Thermal radiation Heat flux density range	10 … 10^4 W/m^2
Range of operating temperature values	300…450 K
Emissivity	0.040…0.99

Experimental studies of various coatings of energy-efficient glasses have been conducted. Results presented in Table 4.

Figure 8. Measurement System RGU-2 for calibrating the heat flux sensors and measuring the emissivity of coatings and material surfaces

Table 4. Experimental Results

Material	Emissivity ε
Glass:	
k - glass	0,23
i - glass	0,11…0,12
Films:	
"Solis-85"	0,38
"Solar-guard 35"	0,31
"Solar-guard 50"	0,35
"Heat mirror 77"	0,071
"HPR	0,045

5. Conclusions

A Simulation model for calculating heat exchange in the cavity of a cylinder is developed in relation to the modeling the calibration heat flux sensors and measurement of the emissivity of coatings and material surfaces. The model includes radiant, convective and conducting heat exchange.

It is shown that the convective and conductive components play a small role in the overall heat exchange (up to 0.1%), and their contribution can be neglected.

The radial distribution of heat flow is practically the same for experiments and calculations.

A good coincidence of the experiment results and calculations is obtained for a variant where the emissivity of the sensor and the rest of the bottom surface of the cylinder is $\varepsilon = 0{,}95$. In the central zone of the bottom heat exchanger with a radius of 63% of the radius of the side polished cylinder, the uneven distribution of the heat flux does not exceed ± 2%, and this zone is suitable for measurements. Taking into account the difference emissivity of the sensor and the rest of the lower surface leads to an increase in heat flow, but this increase is negligible, and amounts to 3.8… 3.9%

Modernized the measurement system RGU-2 for calibrating the heat flux sensors and measuring the emissivity of coatings and material surfaces.

Experimental studies of various coatings of energy-efficient glasses have been conducted.

6. Acknowledgments

These researches have been performed within of the scientific program «Semiconductor Materials, Technologies and Sensors for Technical Diagnostics, Control and Control Systems» by the project TD 15/1.7.1.885 «Creation and implementation devices for controlling the emission coefficient of materials and coatings using highly sensitive infrared sensors»

REFERENCES

1. ZHANG L., CHEN R. (2004). TiO2-Siloxane Thermal Control Coatings for Protection of Spacecraft Polymers. Chinese Journal of Aeronautics, Vol.17, Iss. 1, pp. 53-59. Retrieved from: doi:10.1016/S1000-9361(11)60203-3
2. FINCKENOR M., DOOLING, D. (1999). .NASA/TP-1999-209263. Multilayer Insulation. Material Guidelines. Alabama: Marshall Space Flight Center. Retrieved from: *https://ntrs.nasa.gov/archive/nasa/casi.ntrs.nasa.gov/19990047691.pdf*
3. GILMORE D. (2002). Spacecraft Thermal Control Handbook. The Aerospace Press. 836p. Retrieved from: https://www.amazon.com/Spacecraft-Thermal-Control-Handbook-Technologies/dp/188498911X#reader_188498911X.
4. FREELAND R., BILYEU G., VEAL G. (1996). Development of flight hardware for a large, inflatable-deployable antenna experiment. Acta Astronautica. v.38. I 4 - 8. pp. 251-260. Retrieved from: https://doi.org/10.1016/0094-5765(96)00030-6.
5. BABAK V., KOVTUN, S. Calibration of thermoelectrical heat flux sensors in systems for diagnosing the thermal state of electric machines. Technical Electrodynamics, № 1, 2019. P.89–92. DOI: 10.15407/techned2019.01.089
6. DINZHOS, R., FIALKO N., LYSENKOV E. «Features of thermal conductivity of composites based on thermoplastic polymers and aluminum particles» Journal of nano-and electronic physics. Vol.7 No 3, 03022 (4pp) (2015).
7. ISACHENKO V., OSYPOVA V., SUKOMEL A. (1975) «Heat transfer» Textbook for universities,3-d ed., 488 p.
8. KRÁLÍK T., MUSILOVÁ V., HANZELKA P., FROLEC J. (2016). Method for measurement of emissivity and absorptivity of highly reflective surfaces from 20 K to room temperatures/ Metrologia. 53, 743–753. Retrieved from: doi:10.1088/0026-1394/53/2/743
9. BABAK V., VOROBIOV L., DEKUSHA L., VOLKOV V., BUROVA Z., DEKUSHA O., KOVTUN S. (2018). Calorimetric methods for monitoring the thermal characteristics of energy-efficient coatings. Bulgarian Society for NDT: International Journal “NDT Days”, V. 1, Is. 2, 2018. - C. 203 - 212.
10. MARUKOVYCH E., MARKOV A. BONDAREV O. (2011). Remote flaw detection of contour surfaces. Mynsk, Belarus Navuka. 330 p.

11. BABAK V., DEKUSHA O., VOROBIOV L., KOBZAR S., IVANOV S. The Heat Exchange Simulation In The Device For Measuring The Emissivity Of Coatings And Material Surfaces. 2019 IEEE 39th International Conference on Electronics and Nanotechnology, ELNANO 2019 - Proceedings Retrieved from: *https://ieeexplore.ieee.org/xpl/conhome/8767103/proceeding*